



Air Flow Analysis and Effect of Angle on Rotation Vane Blade through 90 Degree by Computational Fluid Dynamic

Muhammad Asyraf Masuri¹, Mohd Yussni Hashim^{1*}

¹ Faculty of Mechanical and Manufacturing Engineering,
Universiti Tun Hussein Onn Malaysia, Batu Pahat, 86400, MALAYSIA

*Corresponding Author

Received 14 December 2022;
Accepted 15 January 2023;
Available online 1 March 2023

Abstract: This article presents the result of Computational Fluid Dynamics (CFD) simulations of airflow velocity and pressure distribution at two types of rotation vane at a 90-degree pipe bend: (1) 10° rotation vane blade angle and (2) 33° rotation vane blade angle in 0.1m pipe cross-section. The pressure drops of the two rotation vanes were also calculated for comparison. The CFD-based empirical model can predict the velocity and pressure of the pipelines model, with the modeling results validated by a previous study. The input parameters to ANSYS Fluent are viscosity, density, and inlet fluid velocity of 10m/s to 30m/s, and the output of the computer simulation is velocity and pressure at two different sections. The simulation results were taken in two sections: (1) A-A and (2) B-B, and each section consisted of 10 points across the cross-section of the pipe with a 0.01m distance between two-point.

Keywords: Rotation Vane, Pipe Bend, Velocity Profile, Pressure Drop

1. Introduction

In general, fluid can be classified into two different substances which are liquid or gas. The fluids will be flowing and change in shape at a steady rate according to the direction of the force that is applied. These characteristics allow the fluids easier to flow from one location that is commonly used in the pipelines system [1,2]. The high-velocity fluid that significant changes in direction due to the pipe bend may cause wear to the wall of the pipe that has low material strength [3-5]. The flow of incompressible viscous fluids through pipe bends is characterized by flow separation, secondary flow, and unsteadiness which are dependent on Reynolds number which can determine whether the type of flow such as laminar and turbulent. The fluid that experienced turbulent flow can increase the rate of shear stress along the pipe due to the existence of secondary flow in the bends [6].

Furthermore, the pressure will occur at the cornering pipe because of the fluid that hits the bend and changes the direction thus can cause corrosion at the bend of the pipelines. The flow rate, static pressure, and wall shear stress influenced corrosion distribution due to secondary and separating flows [7-9].

The problem can be solved by using the rotation vanes to assist the fluid flow in making a smoother and more gradual change in direction, resulting in less impact and pressure drop [10]. This type of vane can reduce the pressure drop through an elbow, turns fluid turbulence to laminar, and prevent fluid separation. It also improves the flow of fluid through any type or angle of the elbow and creates a smooth aerodynamic flow to ensure full rotation of all components in the fluid. A study has been made by Mutsakis [11], towards experimental approach to define the flow pattern of the fluid with various angle of rotation vane.

In this study, the use of rotation vane with a different type of vane angle is used to produce rotation to the fluids before and after passing through the pipe bend to reduce the turbulence of the fluid as it passes through the curve pipe section. The numerical simulations that using computational fluid dynamics (CFD) were conducted with two different pipeline models to determine the best angle of rotation vane blade in terms of velocity, pressure distribution and, pressure drop [12].

2. Methodology

The numerical simulations were carried out based on R18.2 version of ANSYS Fluent with various subroutines add on to model moving mesh and boundary capability to replicate the real pipelines and rotation vane conditions, such as materials, density, and a viscosity [13]. The development of models started from the design of the pipelines by using SolidWorks software and the simulation carried by ANSYS Fluent software would provide good accurate results.

2.1 Governing equations

In this study, equivalent formulations have been calculated by CFD for incompressible multi-fluid flow including the effects of density and viscosity. The formal controlling the motion of unsteady, viscous, incompressible, immiscible two-fluid systems are the equations of Navier-Stokes [14,15]. The 3D Reynolds Averaged Navier-Stokes (RANS) equations are solved using the segregated implicit solver. The governing equations for incompressible fluid flow with constant properties are as follows.

$$\frac{\delta u_i}{\delta x_i} = 0 \quad (1)$$

$$\frac{\delta u_i}{\delta t} + u_j \frac{\delta u_i}{\delta x_j} = f_i - \left(\frac{1}{p} \frac{\delta p}{\delta x_i} \right) + \nu \frac{\delta^2 u_i}{\delta x_j \delta x_j} \quad (2)$$

Equations 1 and 2 are the conservations of mass and momentum, where f_i is a vector representing external force, ν is the kinematic viscosity. The turbulent model used was realizable k -epsilon due to the more accurate prediction and the k -epsilon model performs better for single-phase flows in pipe bend. The turbulence kinetic energy (k) and the turbulence dissipation rate (ϵ) are solved and calculated by CFD to determine the coefficient of turbulent viscosity (μ_t).

$$\frac{\delta(pk)}{\delta t} + \frac{\delta(pk u_i)}{\delta x_i} = \frac{\delta}{\delta x_j} \left(\frac{\mu_t}{\sigma_k} \frac{\delta k}{\delta x_j} \right) \quad (3)$$

$$+ 2\mu_t E_{ij} E_{ij} - \rho \epsilon$$

$$\frac{\delta(\rho \epsilon)}{\delta t} + \frac{\delta(\rho \epsilon u_i)}{\delta x_i} = \frac{\delta}{\delta x_j} \left(\frac{\mu_t}{\sigma_\epsilon} \frac{\delta \epsilon}{\delta x_j} \right) \quad (4)$$

$$+ C_{1\epsilon} \frac{\epsilon}{k} 2\mu_t E_{ij} E_{ij} - C_{2\epsilon} \rho \frac{\epsilon^2}{k}$$

From the above equations, u_i represent velocity component in the corresponding direction, E_{ij} represent a component of the rate of deformation, μ_t represent eddy viscosity. The equations 3 and 4 also consist of some adjustable constants which are $C_\mu = 0.09$, $\sigma_k = 1.00$, $\sigma_\epsilon = 1.30$, $C_{1\epsilon} = 1.44$ and $C_{2\epsilon} = 1.9$. The inlet velocity for this study are 8m/s, 10m/s and 12m/s with gauge pressure of 101.325 kPa.

12

Published by FAZ Publishing

<http://www.fazpublishing.com/jcf>

2.2 Geometry modelling, materials, and phase setup

The fluid flow in pipelines was airflow with different velocities (10,14,20, 24, 26, and 30 m/s), 1.225 kg/m³ air density and 0.000017894 kg/m.s viscosity. The rotation vane blade was declared as solid (Steel) with 8030 kg/m³ density while the operating pressure was set as atmospheric pressure. All the results in this study were taken at section A-A and section B-B along (P1-P10) where P1 to P5 is the lower part and P5 to P10 are the upper part shown in figure 1. The bottom vertical part of the pipe as the inlet for fluid to flow and at the end of the horizontal part for the outlet flow.

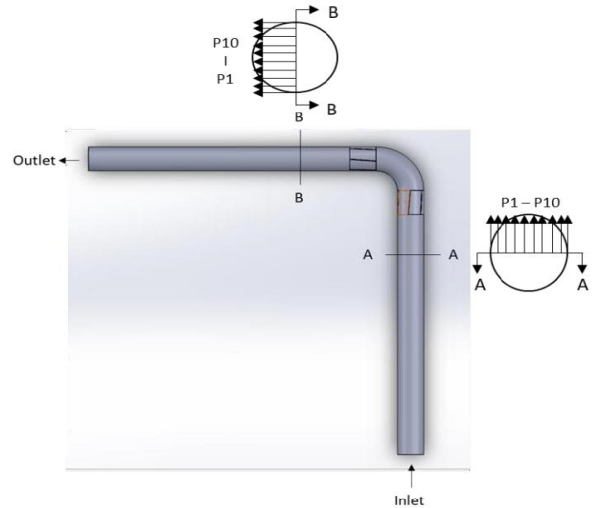


Fig. 1 – Location of section A-A, section B-B and P1-P10

3. Results and Discussion

Two simulations have been conducted that are (1) simulation 1 with a 10-degree rotation vane blade angle and (2) simulation 2 with a 33-degree rotation vane blade angle. Every data has been obtained across the line at different sections that are at (1) section A-A and (2) at section B-B in the post-processing process in ANSYS Fluent. The value of the velocity and pressure can be illustrated by plotting the graph.

3.1 Velocity distribution

Figure 2 and 3 shows the velocity contour at 10m/s velocity inlet for simulation 1 and 2. Figure 4 and 5 show velocity profile at section A-A and section B-B for simulation 1 respectively, while figure 6 shows velocity profile at section B-B for simulation 2.

The velocity graph shows that the velocity increase when the Reynolds number increase. The velocity profile at section B-B for both simulations is irregular in the middle of the cross-sectional pipe than at section A-A due to the presence of rotation vane that act as barrier for fluid to flow. The maximum velocity for section A is at the centre of the pipe cross-section, while equal to zero at the wall due to the viscosity of fluid that sticks at the pipe wall. For sections B-B, the maximum is at the P9 which is the upper part of the pipe model.

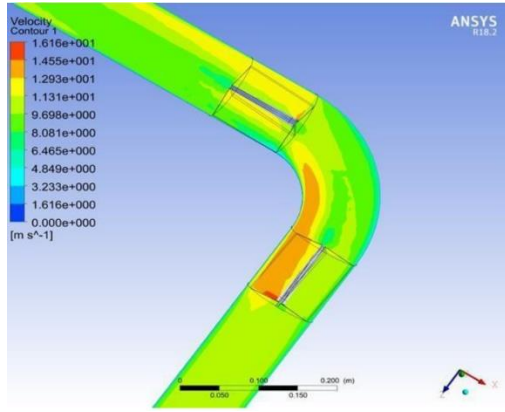


Fig. 2 – Velocity contour for simulation 1

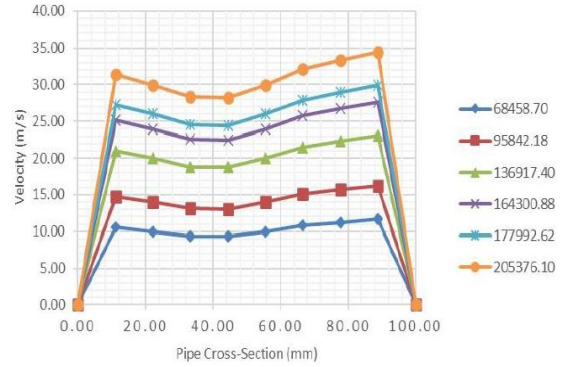


Fig. 7 – Velocity distribution simulation 2, cross section B-B

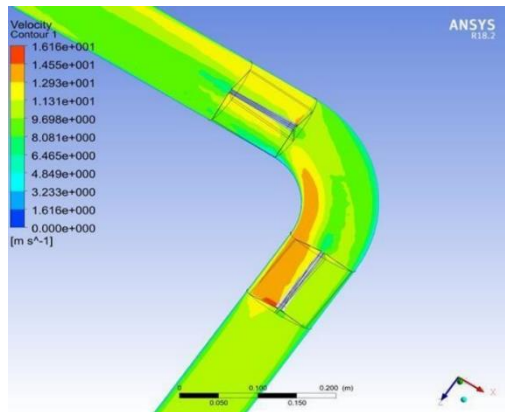


Fig. 3 – Velocity contour for simulation 2

3.2 Pressure distribution

Figure 8 and 9 shows the pressure contour at 10 m/s velocity inlet for simulation 1 and 2. Figure 10 and 11 show pressure profile at section A-A and section B-B for simulation 1 respectively, and figure 12 shows pressure profile at section B-B for simulation 2.

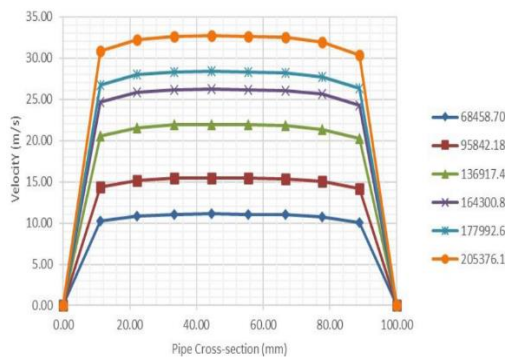


Fig. 4 – Velocity distribution for cross section A-A

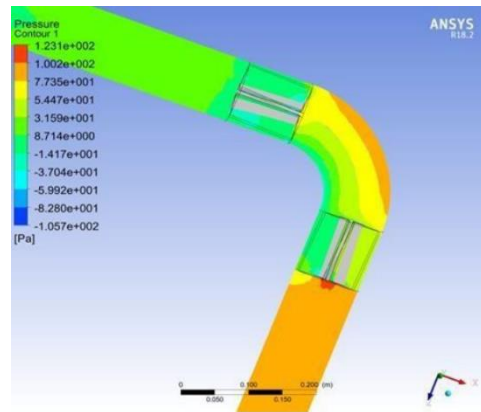


Fig. 8 – Pressure contour for simulation 1

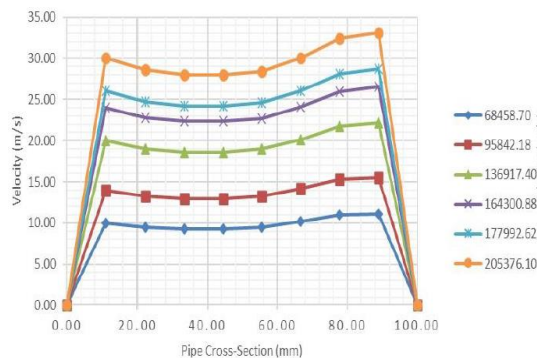


Fig. 5 – Velocity distribution simulation 1, cross section B-B

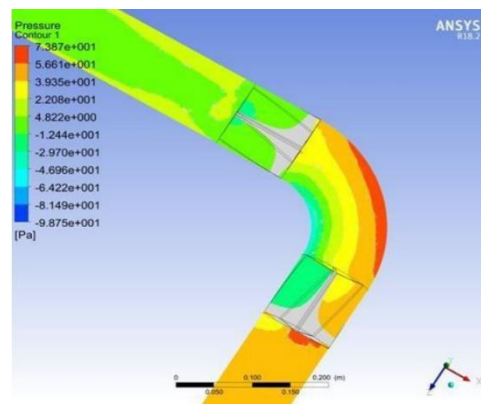


Fig. 9 – Pressure contour for simulation 2

The pressure graph shows the opposite trend of pressure distribution with a velocity profile. This is due to the momentum exchanges and normalized pressure from the uniform value of static pressure before the fluid passes through the rotation vane blade to the curvature of the pipe bend.

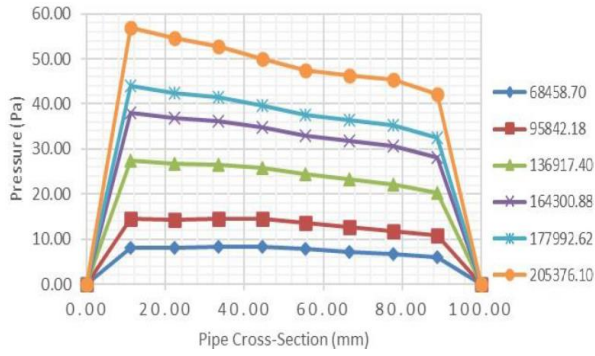


Fig. 10 – Pressure distribution sim. 1, cross section A-A

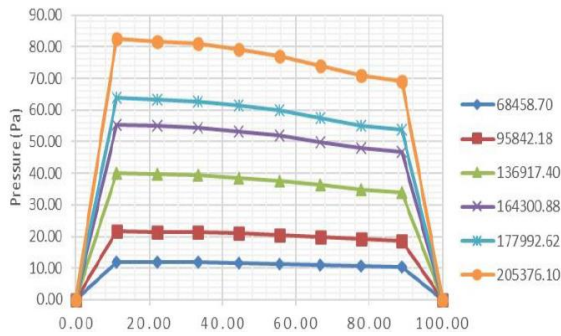


Fig. 11 – Pressure distribution sim. 1, cross section B-B

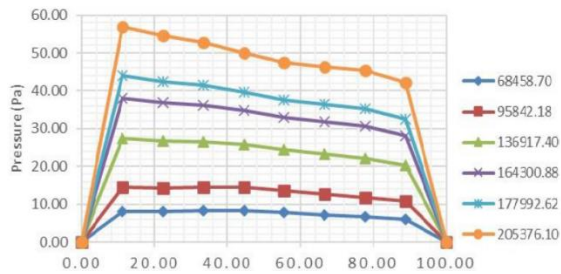


Fig. 12 – Pressure distribution sim. 2, cross section B-B

The pressure from lower to upper part at section B-B for both simulation results show that the pressure experience slightly drops under the impact of the centrifugal force resulting from the circular motion of fluid particles induced by the curvature of the pipe bend [4]. The pressure distribution at simulation 2 is lower than at simulation 1 due to the presence of different geometry of rotation vane blade. The larger angle of rotation vane blade will act as a larger barrier for fluid to thus resulting in the pressure to be reduced.

3.3 Pressure drop

Figures 13, 14 and 15 show the comparison of the velocity, pressure, and pressure drop between 10° and 33° rotation vanes, respectively. The highest Reynolds number was taken for comparison. The graph shows that 33° rotation vane developed higher velocity, pressure, and pressure drop than 10° rotation vane.

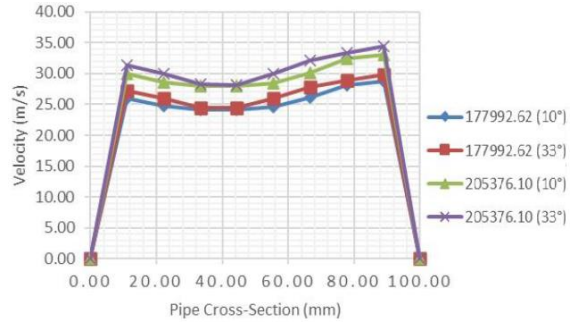


Fig. 13 – Comparison of velocity distribution

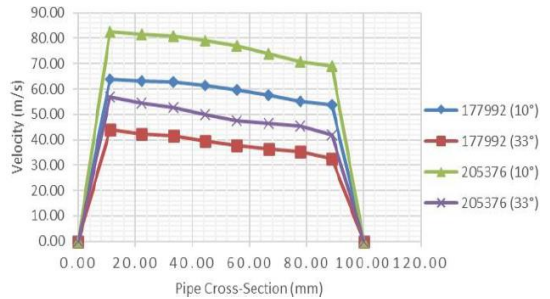


Fig. 14 – Comparison of pressure distribution

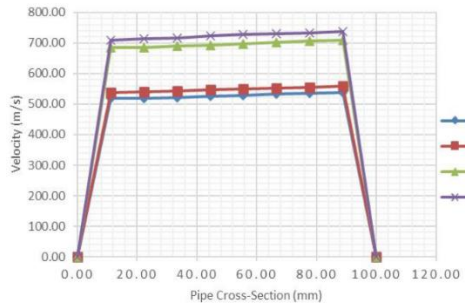


Fig. 15 – Comparison of pressure drop

4. Conclusion

All the result of this study has successfully achieved the requirements outline of the objective. The conclusions are made based on both simulation results where the air that acts as the fluid to flow along the pipe model show that as the Reynolds number increase, the velocity, the pressure distribution, and the pressure drop will increase for every pipe model. The pressure distribution along the pipe model is inversely proportional to the velocity profile. These results are obeying the theory of the momentum equation that consists of potential energy, kinetic energy, and pressure. As the velocity that presents in kinetic energy increases, the pressure must reduce correspondingly to keep all the points along a streamline constant. In conjunction, when the fluid passes through the pipe bend, the pressure tends to reduce and resulting in the velocity to increase.

Therefore, the pressure drops occurred at many pipe bends in the pipelines system. The velocity, the pressure, and the pressure drop of the fluids that pass through the 10-degree rotation vane blade angle is lower than the 33-degree rotation vane blade angle at the discharge point (Section B-B). As for the conclusion, the separation flow can be eliminated by installing the rotation vane at pipe bend in the pipelines system and the best angle for rotation vane blade angle is 10-degree due to the lower pressure drop that can give higher efficiency of the flow system.

References

- [1] Tanaka, M.A., Ohshima, H., and Monji, H., "Numerical investigation of flow structure in pipe elbow with large eddy simulation approach." in: *ASME 2009 Pressure Vessels and Piping Conference, American Society of Mechanical Engineers*, (2009): 449-458
- [2] Barros Galvis, N. "Geomechanics, Fluid Dynamics and Well Testing, Applied to Naturally Fractured Carbonate Reservoirs, Springer, 2019.
- [3] Dutta, P., Saha, S.K., Nandi, N., and Pal, N., "Numerical study on flow separation in 90° pipe bend under high Reynolds number by k-ε modelling." *Eng. Science and Technology*. 19(2) (2016): 904- 910.
- [4] Karimipour, A., Afrand, M., Akbari, M., and Safaei, M.R., "Simulation of fluid flow and heat transfer in the inclined enclosure." *Int. J. Mech. Aerosp. Eng*, 6 (2012): 86-91.
- [5] Homicz, G.F., "Computational Fluid Dynamic Simulations of Pipe Elbow Flow." *Department of Energy*, USA (2004)
- [6] Jones, J Lloyd, Kosla, A., Lee "Eliminating Elbow Exit Flow Distortion and its Effect on Downstream Check Valves." Presented at the *Nuclear Industry Check Valve Group*, Winter meeting, 1992.
- [7] Khadijah Binti Asus. "Air Flow Analysis and Effect of Angle on Rotation Vane Blade Through 90 Degree Pipe Bend." Universiti Teknologi Malaysia, Johor Bahru: Tesis Ijazah Sarjana Muda.
- [8] Lin, C.H., Ferng, Y.M., "Predictions of hydrodynamic characteristics and corrosion rates using CFD in the piping systems of pressurized water reactor power plant." *Ann Nucl Energy*, 65 (2014):214-222.
- [9] Mazumder, Q.H., "CFD Analysis of the Effect of Elbow Radius on Pressure Drop in Multiphase Flow." *Modelling And Simulation in Engineering*, 12 (2012): 1-8.
- [10] Azzi, A and Friedel, L., "Two-phase upward flow 90° bend pressure loss model." *Forschung im Ingenieurwesen*, 69(2) (2005): 120–130.
- [11] Mutsakis et al. "Laminar Flow Elbow System and Method." U.S. Patent 19. 5, 529, 084. 1996.
- [12] Rowe, M., "Measurement and computation of flow in pipe bends." *Journal of Fluid Mechanics*, 43(77) (1970): 783. DOI: 10.1017/S0022112070002732.
- [13] Moujaes, S.F., and Aekula, S., "CFD predictions and experimental comparisons of pressure drop effects of turning vanes in 90° duct elbows," *Journal of Energy Engineering*, 135(4) (2009): 119–126.
- [14] Saha, S., and Nandi, N., "Numerical Study about the Change in Flow Separation and Velocity Distribution in a 90o Pipe Bend with/without Guide Vane Conditions." *International Journal of Technology*, 8(4) (2017): 681.
- [15] Yugasunthran A/L P.Mohan., "Air Flow Analysis and Effect of Angle on Rotation Vane Blade Through 90 Degree Pipe Bend." Universiti Teknologi Malaysia, Johor Bahru: Tesis Ijazah Sarjana Muda.

Acknowledgement

The authors would also like to thank the Faculty of Mechanical and Manufacturing Engineering, Universiti Tun Hussein Onn Malaysia, and Advanced Forming Research Group for its support.